Characterizing Species Composition in Radio-Frequency Plasma Produced from Water Vapor

IEPC-2007-082

Presented at the 30th International Electric Propulsion Conference, Florence, Italy
September 17-20, 2007

Sonca Nguyen*, Kristina Lemmer†, John Foster‡, and Alec Gallimore§
University of Michigan, Ann Arbor, Michigan, 48109, USA

Abstract: Using hydrogen as an energy carrier has the potential to address the need to reduce oil consumption and pollution. However, hydrogen is only as clean as the method employed for its production. This work experimentally investigates an unconventional method of hydrogen production by breaking up water molecules in a radio-frequency plasma. This paper demonstrates that this proposed method can successfully dissociate water molecules and presents some characteristics of the RF plasma produced from water vapor including floating potential, ion saturation current, and partial pressures of the gases. Of most relevance to the goal of this project is the hydrogen partial pressure, and it is shown that for the same vacuum facility pumping speed, operating the RF plasma source at increased pressure and mass flow rate produces less hydrogen. For the same mass flow rate and at RF power greater than 1000 watts, the partial pressure of hydrogen to total pressure is higher for lower chamber pressure.

I. Introduction

ONE present global challenge is to reverse the growing dependence on oil while reducing pollution and greenhouse gases. Carbon dioxide (CO_2) emissions are rapidly increasing as consumption of natural resources increases worldwide. Two important reasons for addressing this challenge include the limited future natural resources and the strong correlation between CO_2 emissions and global temperature increase. For some countries, the need to reverse growing national dependence on oil ties with national energy security. For example, in the United States, the country's energy security is threatened by its dependence on foreign oil, which constituted 58% of the oil consumed in the U.S. in 2005.[1] Of the 20.6 million barrels of oils consumed by Americans each day in that same year, 2/3 went to the transportation sector. One proposed solution is to develop the technology for commercially viable hydrogen-powered fuel cells to power cars, trucks, homes, and businesses with no pollution or greenhouse gases.[2]

As fuel cell technology matures, efficient hydrogen production is equally important to complete a clean energy cycle. Hydrogen is the most abundant element in the universe, but it rarely exists in its natural form on this planet. Hydrogen, therefore, is not an energy source, but an energy carrier. Therefore, it will be only as clean as the method employed for its production. Currently, 98% of hydrogen is produced from reforming of fossil fuels and is used mainly in oil refining, and ammonia and methanol production.[3] To address the previously stated challenge fully, hydrogen production needs to be a renewable process, using only renewable resources such as water. Electrolysis is currently the dominant renewable method of hydrogen production. However, this technique has approximately 25% energy efficiency when including the electricity efficiency and it also requires expensive catalysts.[4]

* Graduate Student, Aerospace Engineering, sonca@umich.edu.
† Graduate Student, Aerospace Engineering, klemmer@umich.edu.
‡ Professor, Nuclear Engineering and Radiological Sciences, jefoster@umich.edu.
§ Professor, Aerospace Engineering, alec.gallimore@umich.edu.

This paper experimentally investigates a new technique of hydrogen production using a radio-frequency (RF) plasma source. Similar to electrolysis, hydrogen is produced from water in this proposed method. The electron temperature is expected to be of a few electron volts and the density can be in a range between 10^{17} to 10^{19} m^{-3} depending on which mode (capacitive, inductive, or helicon) the plasma operates in. Among these modes, helicon mode is most energy efficient. Consequently, highly reactive species in the plasma including electrons, ions, and radicals are speculated to enhance the water dissociation rate. Unlike electrolysis, catalysts are not required. Previous works have recognized the promising potential of plasma for hydrogen production, but have used plasma to break up only hydrocarbons or have used it in a form of a catalyst.[5-9] One group has attempted to dissociate water molecules in a steam-plasma torch powered by microwaves.[10] Characteristics of the plasma produced from water vapor, specifically from a RF source, are not available to our knowledge. This paper characterizes the ion saturation current and floating potential of the RF plasma source for both argon and water. As a step toward characterizing the efficiency of this proposed method, partial pressures of H_2, O_2, OH, and H_2O are presented for a wide range of operating conditions of RF power and magnetic field strength.

II. Experimental Setup

A. Vacuum Facility

The plasma source is attached on a side port of a cylindrical chamber that is 2 m long and 0.6 m in diameter. An Edwards 2-Stage pump is used to evacuate the chamber. When the mechanical pump is operated alone, the chamber pressure typically continues to decrease below 50 mtorr. Gas flown into the chamber maintains a pressure of at least 50 to 70 mtorr to prevent backstreaming. The chamber is also fitted with a CVI 20-inch (51-cm) cryopump, which can bring the base pressure to $3x10^{-7}$ torr. Figure 1(a) shows the main cylindrical vacuum chamber with its pumps attached along with the plasma source and the three magnet coils. For argon, when the cryopump is used, the chamber pressure is 1 mtorr for a 240 sccm flow rate. With mechanical pumping alone, at an argon flow rate of 40 sccm, the background chamber pressure is 100 mtorr. A linear extrapolation indicates that a chamber pressure of approximately 400 mtorr corresponds to an argon flow rate of 240 sccm. Unfortunately, our water vapor mass flow controller has not worked properly and we have not calibrated the chamber pressure for water vapor. However, we expect that the calibration for water vapor is similar to that of argon.

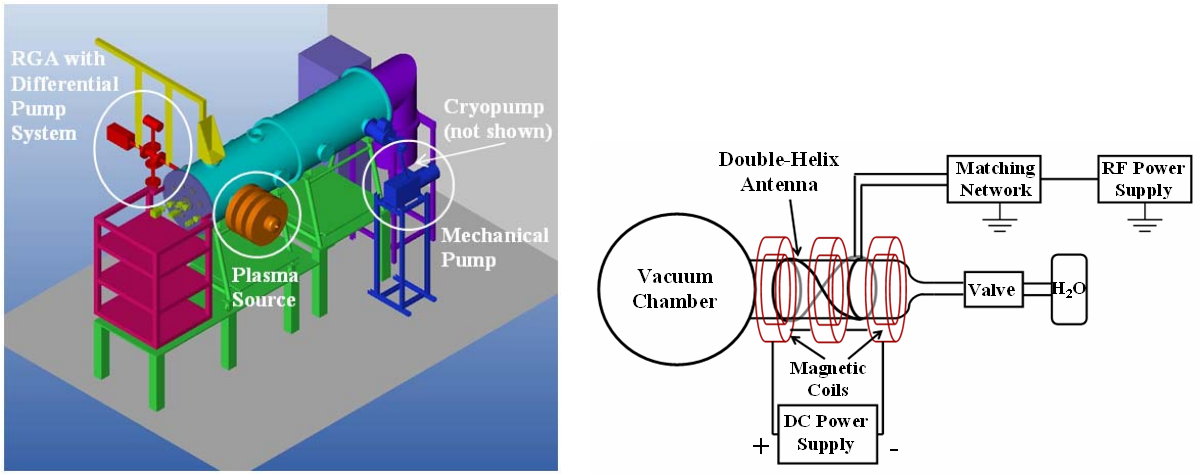

a) **b)**

Figure 1. a) Main vacuum chamber setup. b) Schematic diagram of plasma source.

B. Plasma Source

A schematic diagram of the plasma source, a quartz tube that is 15 cm in diameter and 50 cm in length, is shown in Fig. 1(b). Three magnet coils are used to generate the magnetic field. The coils are connected in series to a 60-A DC power supply. At 60 A, the magnetic field strength near the center of the plasma source is approximately 400 G. A double helical antenna circumscribes the quartz tube, and is sandwiched between the quartz tube and the magnetic

coils. A 13.56 MHz RF power supply excites the antenna up to 3 kW. A π-matching network is used to match the impedance of the RF power supply output with the impedance of the antenna, reducing the reflected power between 2-5% of input power. Water vapor is produced in a separate vessel and is delivered to the plasma source via a mechanical valve.

C. Residual Gas Analyzer

A Kirk J. Lesker residual gas analyzer (RGA) is used to identify gas species in the plasma, as well as, to measure their partial pressures inside the main chamber. The RGA's operating pressure limit is 10^{-4} torr while the chamber pressure is two orders of magnitude higher than this limit when operating with the mechanical pump. A differentially pumped system as shown in Fig. 2(a) is used to allow for RGA operation. The plasma in the main chamber enters the spectrometer chamber through a variable leak valve. A turbomolecular pump from Varian (model V70LP) is used to pump the gases out of the spectrometer chamber, maintaining the pressure of the spectrometer chamber below the RGA pressure limit.

Equation (1) relates the pressure in the spectrometer chamber to the main chamber pressure and facility geometry. The parameter P_s is the pressure of the spectrometer chamber, P_c is the pressure of the main chamber, C is the conductance, and S_p is the pumping speed of the auxiliary system (Fig. 2(a)). This expression is obtained by setting Q_1 equals to Q_2, which equals to S_pP_p, where Q_1 is the throughput in pipe 1 and Q_2 is the throughput in pipe 2, and P_p is the pressure of the pump. Note that the pipe conductances, *C1* and *C2*, are both proportional to the square root of the mass of the gases while S_p depends on the pump type. In order to ensure that the gas in the spectrometer chamber is representative of that in the main chamber, C_2 must be much less than S_p in Eq. (1).[11, 12] This result leads to Eq. (2), where again C_1 and C_2 have the same mass dependency.

$$P_S = \frac{P_c}{1+\left(\frac{C_2}{C_1}\right)\left(\frac{S_p}{S_p+C_2}\right)} \qquad C2<<Sp \qquad (1)$$

$$P_S = \frac{P_c}{1+\left(\frac{C_2}{C_1}\right)} \qquad (2)$$

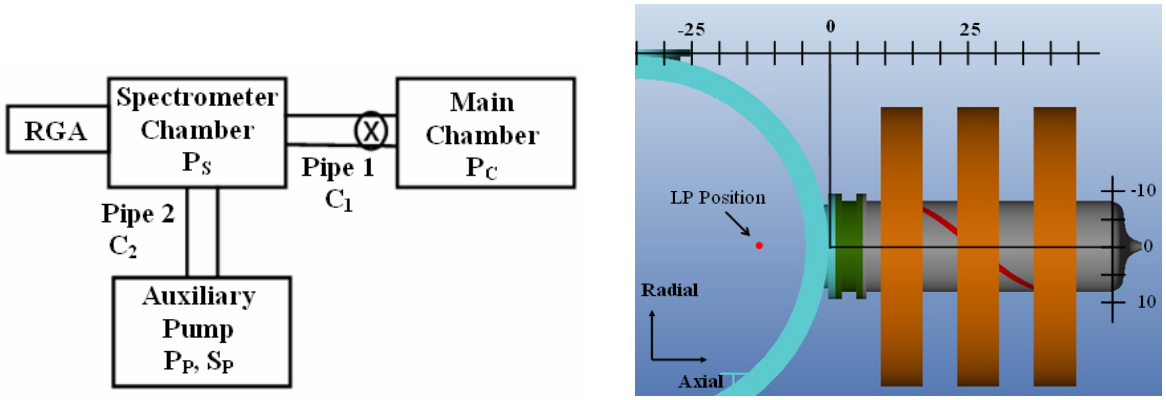

a) b)

Figure 2. a) Schematic diagram of differentially pumped system for the RGA. b) Plasma source with axis definition. *Langmuir probe data are taken at -13 cm in the axial direction.*

D. Langmuir Probe

A commercial Langmuir probe system by Hiden is used to measure ion saturation current and floating potential of the plasma. This probe is RF-compensated. In order to avoid surface contamination on the probe tip, direct heating is applied. Before taking data for each sweep, the probe is set at 100 V for 0.2 s up to 1 s. The probe tip is tungsten and is 10 mm in length and 0.15 mm in diameter. Langmuir probe data shown in this paper are measured at negative 13 cm in the axial direction from the origin as defined in Fig. 2(b). The probe tip is oriented normal to the axial magnetic field. Near the center of the plasma source, 25 cm in the axial direction and 0 in the radial direction, the axial (z-direction) component of the magnetic field, B_z, is approximately 400 G when 60 A DC current is applied to the magnetic coils. B_x and B_y are 4 and 6 G, respectively. At the origin, B_z, B_x and B_y are 70, 1, and 4 G, respectively. The strength of the magnetic field is reduced proportionally to half of the strength at 60 A for the 30-A case. The strength of the magnetic field at -13 cm in the axial direction, where the Langmuir probe data are taken, should be less than the strength at the origin.

III. Results

A. Ion Saturation Current

Ion saturation current as a function of RF power are shown for 0 A (i.e. no applied magnetic field), 30 A, and 60 A for argon plasma and water plasma. Figure 3(a) shows results for 1 mtorr chamber pressure and Fig. 3(b) shows similar results for 100 mtorr. The cryopump was used to bring the chamber pressure to 1mtorr with a flow rate of 240 sccm, whereas only the mechanical pump was used to maintain 100 mtorr chamber pressure with a flow rate of 40 sccm for argon.

For argon plasma, Fig. 3(a) shows that the ion saturation current is higher when the magnetic field is applied. However, it shows that the ion saturation current is not necessarily a linear function of magnetic field. Contrary to our speculation, the ion saturation current is lower at 60 A than at 30 A. Nonetheless, the results show that the ion saturation current is higher when there is a magnetic field. This trend is also observed in the water plasma. The ion saturation current at 30 A for water is consistently higher than that at 60 A. In comparison with argon, ion saturation current for water is consistently lower by a factor of 3 or 4. All the trends observed at 1 mtorr are also seen in the 100-mtorr case with the exception that the difference in the ion saturation current between 30 A and 60 A is minimal for argon. There is a clear difference in ion saturation current for argon plasma with and without a magnetic field. Similar to the 1-mtorr case, the ion saturation current of argon plasma is a few factors higher than that of the water plasma.

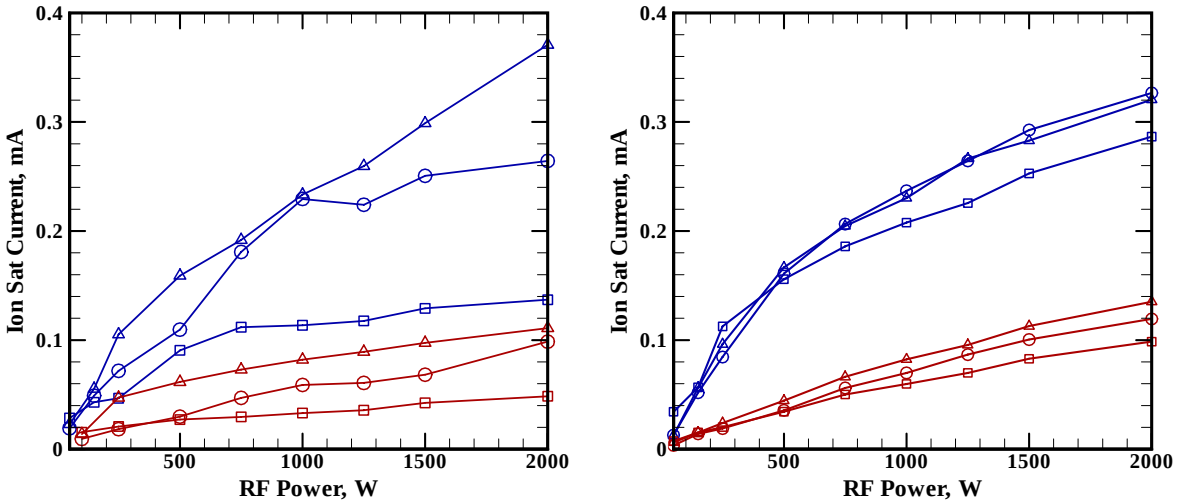

Figure 3. Ion saturation current versus RF power for a) 1 mtorr chamber pressure and b) 100 mtorr chamber pressure. Applied DC current to the magnetic coils are 0 A (square), 30 A (triangle) and 60 A (circle) for argon (blue lines) and water vapor (red lines).

Why the ion saturation current at 30 A is higher than at 60 A at 1 mtorr is at present not well understood. Increased reflected power was ruled out as matching was similar at both conditions. It is possible that a mode jump could have occurred in increasing the magnetic field strength. In this case, assuming the electron temperature does not change, then the larger ion current at 30 A may be due to an increase plasma production due to enhanced coupling efficiency. Still another possibility has to do with cross field diffusion, as the magnetic field strength increases, radial losses decrease, thereby leading to better confinement and increased plasma production. If the magnetic field continues to increase however, radial diffusion to the probe will necessarily decrease in accordance with the decreasing cross field diffusion coefficient. Indeed the ratio of the ion cyclotron frequency to the neutral collision frequency increases by a factor of 2 in going from the 30-A case to the 60-A case in accordance with the increased magnetic field strength. Clearly ion flux to the probe will decrease as this ratio increases. In this respect, the observed ion saturation current trend may simply be an artifact of the nature of collection at the probe. Future investigations will involve different probe orientation (parallel and normal to B) so that this trend can be better understood.

The difference in ion saturation current between argon plasma and water plasma is anticipated. In the case of the argon plasma, all the energy goes into exciting and ionizing argon in addition to simple diffusion losses to the wall. In the case of the water plasma, the energy goes into dissociating the OH-H bonds and O-H bonds, ionizing the atoms and molecules, and exciting vibrational transitions. In this respect, there are many more energy sinks in the case of the water plasma. The large electron inelastic cross section projected by the molecular species in the water plasma ultimately leads to electron cooling and an associated reduce ionization rate. Since ion saturation current is proportional to the square root of the electron temperature, then the ion saturation current will also decrease. Additionally, electron attachment also physically depletes the free electron number density, making them unavailable to participate in ionization.

B. Floating potential

In addition to ion saturation current, floating potential was also measured for both argon and water plasma. Figures 4(a) and 4(b) characterize the floating potential for both plasmas at 1 mtorr and 100 mtorr. For 1 mtorr, the argon plasma floating potential is approximately 12 to 23 V. The floating potential for argon is lower with the applied magnetic field on than for the case without it. However, the difference between the case with the magnetic field and without it is small for the argon plasma compared to the results with the water plasma. For the water plasma, the floating potential is between 10 and 33 V. The floating potential difference between the 0-A and 60-A cases ranges between 10 and 20 V. The effect of the magnetic field on the floating potential of the water plasma is evident.

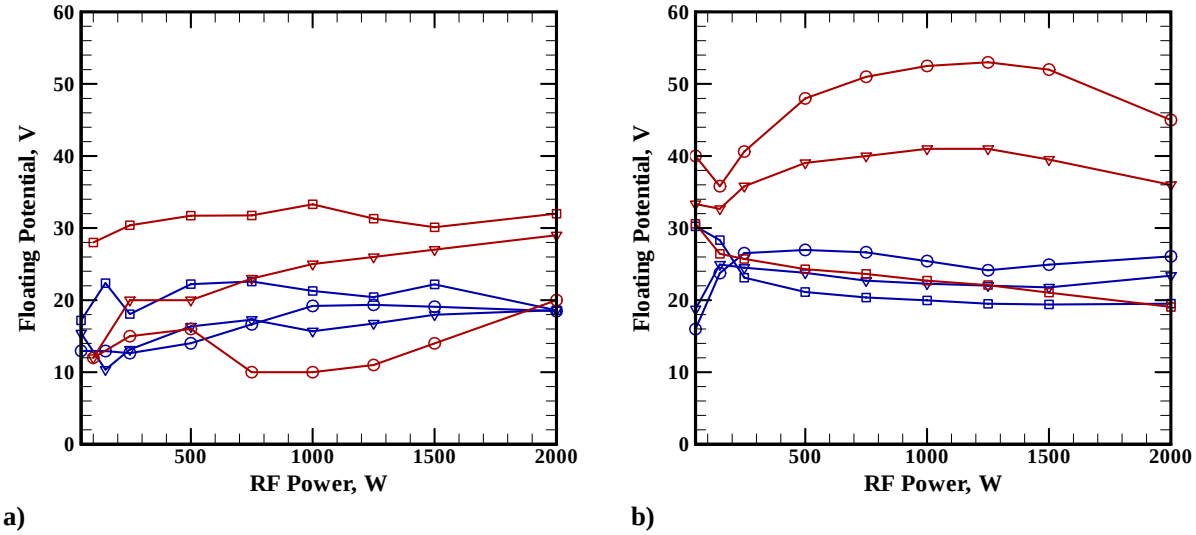

Figure 4. Floating potential current versus RF power for a) 1 mtorr chamber pressure and b) 100 mtorr chamber pressure. Applied DC current to the magnetic coils are 0 A (square), 30 A (triangle) and 60 A (circle) for argon (blue lines) and water vapor (red lines).

At 100 mtorr, the floating potential for argon is consistently around 20 to 25 V. However, the magnetic field has a reverse effect on the floating potential for the water plasma. Without the applied magnetic field, the floating potential for the water plasma falls into the same range as in the argon plasma. However, with the applied magnetic field, the floating potential reaches up to 40 V for 30 A and over 50 V for 60 A. The reason why the floating potential increases to these high values is unclear, but the fact that it is increasing may be an indication that the electron mobility is limited. Several possible explanations for the limited mobility include electron temperature cooling, reduced diffusion coefficient associated with the magnetic field and electron attachment.

C. Species Identification

When water vapor is injected into the RF plasma source, the following species are detected in the plasma: H_2, OH, H_2O, and O_2, with mass/charge of 2, 17, 18, and 32, respectively. Figure 5(a) shows a plot of one set of raw RGA data, which shows the presence of these species. Figure 5(b) shows a picture of the water plasma. The raw RGA data and the color of the plasma demonstrate that the water molecules are dissociated in the plasma source into its constituent parts, hydrogen and oxygen. The next sections characterize the partial pressure of the species as a function of RF power and magnetic field strength.

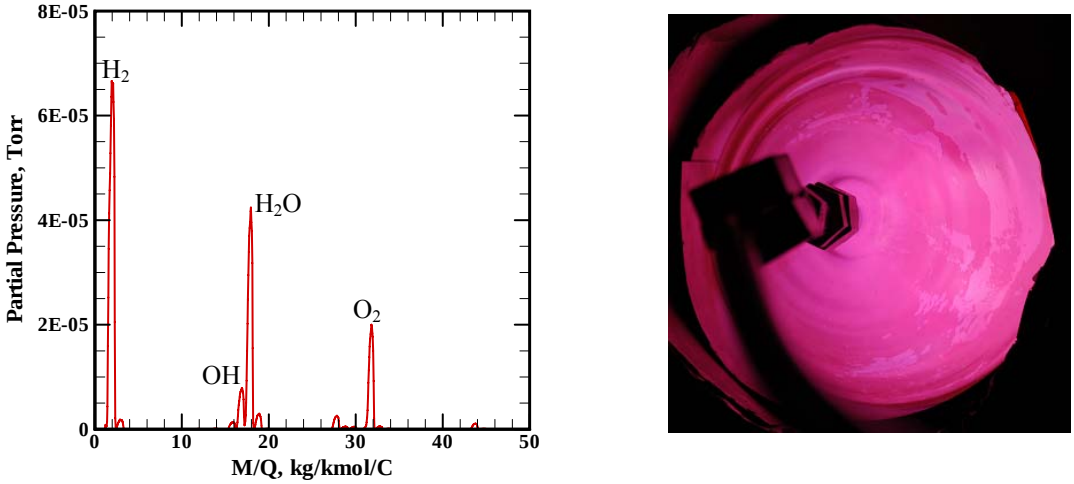

Figure 5. a) A sweep of raw RGA data. b) Picture of water plasma at 1 mtorr, 60 A, and 1.5 kW.

D. Effects of RF power and magnetic field on gas partial pressures

Figure 5(a) shows the raw RGA data, where the partial pressure is calibrated for N_2. In order to obtain a more accurate partial pressure measurement of each species, the ionization sensitivity for each gas relative to nitrogen is taken into account. These values are 0.44, 0.86, and 0.9 for H_2, O_2, and H_2O, respectively.[13] The relative sensitivity for OH is estimated to be similar to that of H_2O, which is 0.9. Figure 6(a) shows the partial pressure normalized to the total pressure for all four species detected in water plasma at 1 mtorr. At this pressure, the magnetic field affects the partial pressure of the gases as more water molecules are dissociated at higher magnetic field strength settings as expected. Consequently, the partial pressure of H_2 is higher with higher magnetic field strength. At 60 A, the partial pressure of H_2 reaches 42% for 2 kW. RF power also affects the composition of the species. The partial pressure of H_2 continues to increase in RF power at all three magnetic field strength settings.

Figure 6(b) shows results for 100 mtorr. The magnetic field and RF power do not affect the composition of the plasma for RF power higher than 1 kW. At lower RF power settings, the results for 30 A and 60 A are indistinguishable, whereas the partial pressure for H_2 is slightly lower with no applied magnetic field. Further, the partial pressure of the gases saturates near 0.5 kW with the magnet and near 1kW without the magnetic field.

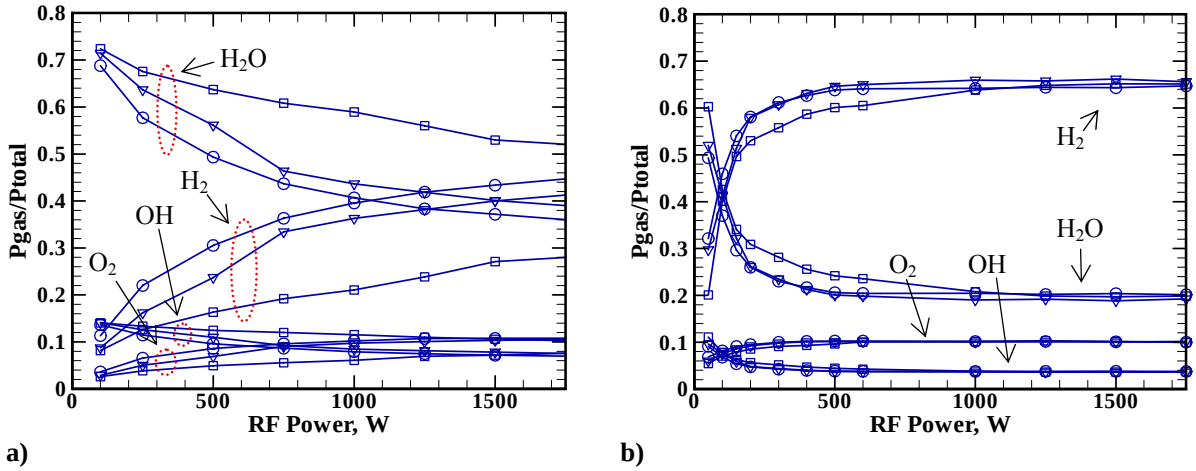

Figure 6. Ratio of H_2, O_2, OH, and H_2O partial pressure to total pressure for a) 1 mtorr chamber pressure and b) 100 mtorr chamber pressure. Applied DC current to the magnetic coils are 0 A (square), 30 A (triangle) and 60 A (circle).

E. Effect of chamber pressure on hydrogen partial pressure

In the previous section, the effects of the magnetic field and RF power on the composition of the plasma are different for different chamber pressures. The value of most interest is the partial pressure of H_2, and this section investigates the effect of chamber pressure on partial pressure of H_2. Figure 7(a) shows results at varying chamber pressures and magnetic field strength settings. Only the mechanical pump was used in this case. Results in Fig. 7(a) reveals that the partial pressure of H_2 decreases with pressure, but are consistently higher with the magnetic field for a given pressure setting. Again, H_2 pressure saturates near 0.5 kW for most cases. An increase in pressure is equivalent to an increase in mass flow rate when the same pump is used. Thus, as the pressure and mass flow rate increase, the percentage of water molecules being dissociated decreases. This result is expected because at a fixed power, adding more gas eventually cools down the electrons, thus saturating the plasma species.

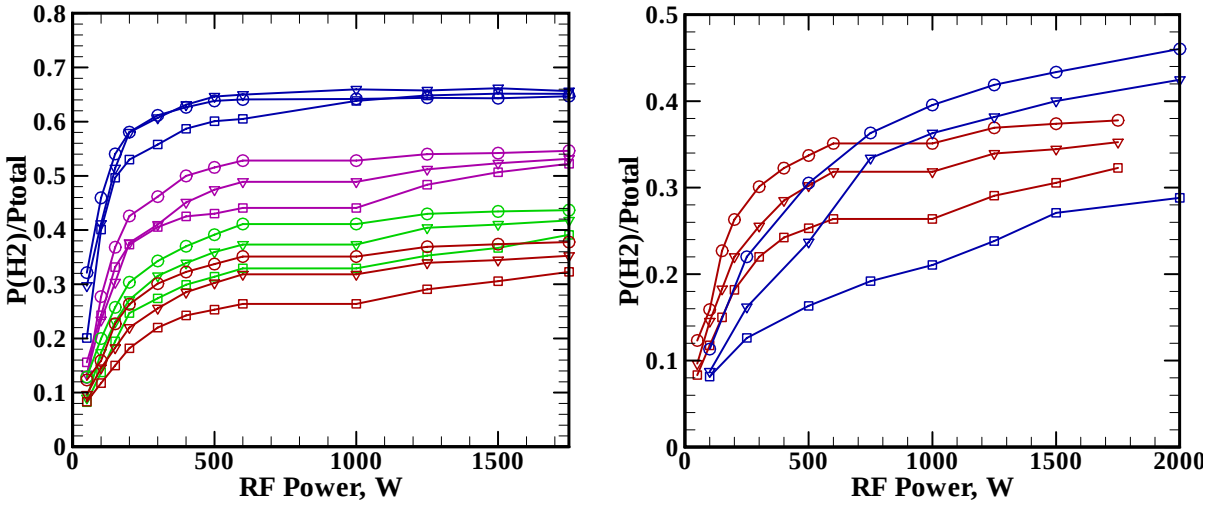

Figure7. Ratio of H_2 partial pressure to total pressure at a) 1 mtorr (blue lines), 200 mtorr (purple lines), 300 mtorr (green lines), and 400 mtorr (red lines) and b) 400 mtorr (red lines) and 1 mtorr (blue lines) chamber pressure. Applied DC current to the magnetic coils are 0 A (square), 30 A (triangle) and 60 A (circle).

Figure 7(b) compares results for two different chamber pressures with the same mass flow rate. A calibration of chamber pressure to flow rate was obtained for argon for both mechanical and cryopump operation. For argon, a chamber pressure of 1 mtorr with the cryopump corresponds to approximately the same mass flow rate as chamber pressure of 400 mtorr with only mechanical pumping. At RF power higher than approximately 750 W and with the applied magnetic field, H_2 partial pressure is higher at 1 mtorr. Below this power, the H_2 partial pressure is higher when operating at 400 mtorr.

One possible explanation for this finding relates to the plasma's different modes of operation. This facility is not expected to operate in helicon mode for argon chamber pressure above 5 mtorr for RF power levels below 1 kW.[14] Therefore, the plasma source can only operate in inductive or capacitive mode at 400 mtorr, whereas there is a possibility that a helicon mode is excited for the 1-mtorr case.

IV. Conclusion

This work has demonstrated the capability of dissociating water molecules in a RF plasma. As a step toward optimizing the efficiency of this method, this paper examines some characteristics of RF plasma produced from water vapor. At 100 mtorr, the floating potential for the water plasma is much higher with the magnetic field than without the magnetic field. Also at this pressure, the magnet and RF power do not affect the composition of the plasma and the H_2 partial pressure saturates above 1 kW. At higher pressure, H_2 partial pressure continues to be unaffected by RF power, whereas the magnetic field affects H_2 production. For approximately the same flow rate but operating in different pressures due to different pumping speeds, a lower pressure is favorable for H_2 production for RF power greater than 1 kW.

Acknowledgments

Sonca Nguyen wishes to acknowledge the National Science Foundation and the Amelia Earhart Foundation for their graduate fellowships. Part of this work is supported by the Hydrogen Energy Technology Laboratory at the University of Michigan, directed by Professor Levi Thompson. The drawings of the vacuum chamber shown in Figs. 1 and 4 were done by mechanical engineering undergraduate student Michael Rayle. Technical assistance from Thomas Griffin from Aerospace Engineering Department is appreciated.

References

[1]"United States Energy Data, Statistics and Analysis - Oil, Gas, Electricity, Coal." URL: http://www.eia.doe.gov/emeu/cabs/Usa/pdf.pdf: [cited 1 July 2007].

[2]"Hydrogen Fuel: A Clean and Secure Energy Future," http://www.whitehouse.gov/news/releases/2003/01/20030130-20.html [cited 1 August 2007].

[3]Marban, G. and Valdes-Solis, T., "Towards the hydrogen economy?" *International Journal of Hydrogen Energy*, Vol. 32, 2007, pp. 1625-1637.

[4]McHugh, K., "Hydrogen Production Methods," MPR Associates, February 2005.

[5]Bromberg, L., Cohn, D. R., Rabinovich, A., and Alexeev, N., "Plasma catalytic reforming of methane," *International Journal of Hydrogen Energy*, Vol. 24, 1999, pp. 1131-1137.

[6]Bromberg, L. *et al.*, "System optimization and cost analysis of plasma catalytic reforming of natural gas," *International Journal of Hydrogen Energy*, Vol. 25, 2000, pp. 1157-1161.

[7]Deminsky, M., Jivotov, V., Potapkin, B., and Rusanov, V., "Plasma-assisted production of hydrogen from hydrocarbons," *Pure and Applied Chemistry*, Vol. 74, 2002, pp. 413-418.

[8]Sobacchi, M.G., *et al.*, "Experimental assessment of a combined plasma/catalytic system for hydrogen production via partial oxidation of hydrocarbon fuels," *International Journal of Hydrogen Energy*, Vol. 27, 2002, pp. 635-642.

[9]Yao, E. Suzuki, S. L., Meng, N., and Nakayama, A., "A High-Efficiency Reactor for the Pulsed Plasma Conversion of Methane," *Plasma Chemistry and Plasma Processing*, Vol. 22, 2002, pp. 225-237.

[10]Uhm, H. S., Kim, J. H. and Hong, Y. C., "Disintegration of water molecules in a steam-plasma torch powered by microwaves," *Physics of Plasmas*, Vol. 14, 2007, pp. 073502-6.

[11]Honig, R. E., "Gas Flow in the Mass Spectrometer," *Journal of Applied Physics*, 1945, Vol. 16.

[12]O'Hanlon, J. F., *A User's Guide to Vacuum Technology*, 3rd ed. Hoboken, NJ: Wiley-Interscience, 2003.

[13]"Cracking Patterns for Gases and Vapours," http://www.hidenanalytical.com/reference/cracking.html [cited 1 July 2007].

[14] Lemmer, K. *et al.*, "Simulating Hypersonic Atmospheric Conditions Conditions in a Laboratory Setting Using a 15-cm Diameter Helicon Source," presented at International Conference on Plasma Science, Albuquerque, New Mexico, USA, 2007.